

AutoMap: Automatic Medical Code Mapping for Clinical Prediction Model Deployment

Zhenbang Wu

University of Illinois at Urbana-Champaign

ZW12@ILLINOIS.EDU

Cao Xiao

Amplitude

DANICA.XIAO@AMPLITUDE.COM

Lucas M. Glass

IQVIA

LUCASMGLASS@GMAIL.COM

David M. Liebovitz

Northwestern University

DAVID.LIEBOVITZ@NM.ORG

Jimeng Sun

University of Illinois at Urbana-Champaign

JIMENG.SUN@GMAIL.COM

Abstract

Given a deep learning model trained on data from a source site, how to deploy the model to a target hospital automatically? How to accommodate heterogeneous medical coding systems across different hospitals? Standard approaches rely on existing medical code mapping tools, which have significant practical limitations.

To tackle this problem, we propose **AutoMap** to automatically map the medical codes across different EHR systems in a coarse-to-fine manner: **(1) Ontology-level Alignment:** We leverage the ontology structure to learn a coarse alignment between the source and target medical coding systems; **(2) Code-level Refinement:** We refine the alignment at a fine-grained code level for the downstream tasks using a teacher-student framework.

We evaluate **AutoMap** using several deep learning models with two real-world EHR datasets: eICU and MIMIC-III. Results show that **AutoMap** achieves relative improvements up to 3.9% (AUC-ROC) and 8.7% (AUC-PR) for mortality prediction, and up to 4.7% (AUC-ROC) and 3.7% (F1) for length-of-stay estimation. Further, we show that **AutoMap** can provide accurate mapping across coding systems. Lastly, we demonstrate that **AutoMap** can adapt to the two challenging scenarios: (1) mapping between completely different coding systems and (2) between completely different hospitals.

1. Introduction

Deep learning models have been widely used in clinical predictive modeling with electronic health records (EHRs) (Xiao et al., 2018). These models often leverage medical codes as an important data source summarizing patients' health status (Choi et al., 2016a,c; Li et al., 2020).

However, in real-world clinical practice, a variety of different coding systems are used across hospital EHR systems (Birkhead et al., 2015). As a result, models trained on data from a source hospital are often hard to adapt to a target hospital where other coding systems are used. A method that can **accommodate different medical coding systems across hospitals for easy model deployment** is highly desirable. Standard approaches rely on existing medical code mapping tools (e.g., Unified Medical Language System (UMLS) (Bodenreider, 2004)), which have significant practical limitations due to the following challenges:

- **Rare coding systems:** Existing commercial and free code mapping tools are only available for a few widely used coding systems (e.g., among ICD-9, ICD-10 and SNOMED CT), as creating such tools requires substantial human efforts (Wojcik et al., 2006). Hospitals using some rare or even private coding systems cannot benefit from the mapping tools.
- **Limited labeled data:** While large hospitals may fine-tune the pre-trained models to adapt to their

coding systems, small hospitals with limited labeled data often fail to do so.

- **No access to source data:** Worse still, the source data usually cannot be shared with the target hospital due to privacy and legal concern.

In this paper, we propose **AutoMap** for automatic medical code mapping across different hospitals EHR systems. **AutoMap** constructs appropriate target embeddings unsupervisedly based on the target EHR data and maps the target embeddings to the source embeddings, so that the deep learning model trained on the source data can be seamlessly deployed to the target data without any manual code mapping. More specifically, **AutoMap** learns the mapping across different coding systems in a coarse-to-fine manner:

- **Embedding.** The medical code embeddings will be constructed from the target EHR data unsupervisedly.
- **Ontology-level Alignment.** We leverage the ontology structure to map medical coding groups via iterative self-supervised learning. In this step, we obtain a coarse mapping matrix from groups of target embeddings to the groups of source embeddings.
- **Code-level Refinement.** We refine the mapping matrix at a fine-grained code level via a teacher-student framework. It utilizes a discriminator (teacher A) to align two coding systems at the code level, and the backbone model (teacher B) to optimize the mapping based on the final prediction.

We evaluate **AutoMap** using multiple backbone deep learning models and test with two real-world EHR datasets: eICU (Pollard et al., 2018) and MIMIC-III (Johnson et al., 2016).

Results show that with a limited set of labeled data, **AutoMap** achieves relative improvements up to 3.9% on AUC-ROC score and 8.7% on AUC-PR score for mortality prediction; and up to 4.7% on AUC-ROC score and 3.7% on F1 score for length-of-stay estimation. Further, we evaluate the mapping accuracy of **AutoMap** and show that **AutoMap** improves the best baseline method by 8.2% in similarity score and 11.3% on hit@10 score. Lastly, we demonstrate that **AutoMap** can still achieve acceptable results under the two challenging scenarios: (1) mapping between completely different coding systems: the model is trained on diagnosis codes and deployed on medication codes;

(2) mapping between completely different hospitals: the model is trained and deployed in hospitals from different regions.

2. Related Work

EHR Representation Learning. Deep learning models have been widely used in EHR representation learning especially for modeling discrete medical codes (Xiao et al., 2018). Existing models were either designed to capture complex and temporal patterns in EHR data (Choi et al., 2016a,b,c; Nguyen et al., 2017; Baytas et al., 2017; Ma et al., 2017; Harutyunyan et al., 2019; Ma et al., 2020a,c; Luo et al., 2020; Zhang et al., 2021a; Xu et al., 2021), model structural information in medical codes (Choi et al., 2017; Shang et al., 2019; Choi et al., 2020), or augment the model using pre-training (Li et al., 2020; Rasmy et al., 2021; Steinberg et al., 2021) and memory network (Shang et al., 2019). However, most of the existing works focus on the model building phase while ignoring the challenge of model deployment due to the diversity of EHR coding formats (Birkhead et al., 2015).

Medical Code Mapping Tools. There exists a variety of commercial and free tools for mapping across different EHR ecosystems. UMLS (Bodenreider, 2004) provides the mapping among ICD-9, ICD-10 and SNOMED CT. Observational Medical Outcomes Partnership (OMOP) (Hripcsak et al., 2015) and Fast Healthcare Interoperability Resources (FHIR) (Mandel et al., 2016) define the standards for representing clinical data in a consistent format. Relying on these tools, some recent works try to support model deployment across hospitals by transforming the EHR data into a standard format (Rajkomar et al., 2018; Tang et al., 2020). However, creating such tools requires a lot of domain knowledge and human labor (Wojcik et al., 2006). These mapping tools are only available for widely-used coding systems and easily outdated due to code updates. To our best knowledge, **AutoMap** is the first work towards code-agnostic deep learning deployment in the healthcare domain without relying on existing code mapping tools.

Transfer Learning. Transfer learning focuses on improving a target task using the knowledge obtained from a model trained for a related source task (Pratt, 1993). Choi et al. (2016b) empirically

confirm that RNN models possess great potential for transfer learning across different hospitals. Gupta et al. (2019) transfer the knowledge with parameter sharing using a deep RNN such that the target task only needs to fine-tune a simpler linear classifier. However, both works assume consistent data format between source and target data. Recently, Ma et al. (2020b) distill knowledge from EHR data to enhance the prognosis for inpatients with emerging infectious diseases. A separate RNN is used for each feature to improve the compatibility across datasets with different feature sets. However, Ma et al. (2020b) still require the availability of both source and target datasets, and a subset of shared features between them. Thus, it does not work in our setting since we only have access to the target dataset with no shared features.

Cross-lingual Word Mapping. Our medical code mapping problem has some similarity to the cross-lingual research. Cross-lingual word mapping methods work by mapping the word embeddings in two languages to a shared space using translation pairs (Artetxe et al., 2017), shared tokens (Søgaard et al., 2018), adversarial learning (Conneau et al., 2018), or the nearest neighbors of similarity distributions (Artetxe et al., 2018).

Inspired by Artetxe et al. (2018), AutoMap also leverages the similarity distributions (Mikolov et al., 2013b) to align medical codes. However, there are significant differences between EHR and natural languages: (1) medical codes often reside in a concept hierarchy; (2) medical codes are often noisier. To address this, instead of directly mapping medical codes, AutoMap adopts a coarse-to-fine method by first performing ontology-level alignment and then code-level refinement.

3. Method

3.1. Problem Setting

We first define a few key concepts, and then present our setting in Prob. 1. Detailed notations can be found in Appx. B.

Definition 1 (EHR Dataset) *In the EHR data, a patient has a sequence of visits: $V_p = [v_p^{(1)}, v_p^{(2)}, \dots, v_p^{(n_p)}]$, where n_p is the number of visits of patient p . For model training, each patient has a label \mathbf{y}_p (e.g., mortality or length-of-stay).*

We will drop the subscript p whenever it is unambiguous. Each visit of a patient is represented by its corresponding medical codes, specified by $v^{(i)} = \{\mathbf{c}_1, \mathbf{c}_2, \dots, \mathbf{c}_{m^{(i)}}\}$, where $m^{(i)}$ is the total number of codes of the i -th visit. Each medical code $\mathbf{c} \in \{0, 1\}^{|\mathcal{C}|}$ is a one-hot vector (i.e., $\|\mathbf{c}\|_1 = 1$), where \mathcal{C} denotes the set of all medical codes in the dataset.

Our setting involves two datasets: a source dataset $*S$ for pre-training the backbone model but unavailable during deployment, and a mostly unlabeled target dataset $*T$ for deploying the model. The two datasets can have completely different medical codes. We also utilize separate medical ontology structures for source and target medical codes.

Definition 2 (Medical Ontology) *A medical ontology \mathcal{O} specifies the hierarchy of medical codes in the form of a parent-child relationship. Formally, an ontology \mathcal{O} is a directed acyclic graph whose nodes are $\mathcal{C} \cup \bar{\mathcal{C}}$. Here, \mathcal{C} is the set of medical codes (often leaf nodes in the ontology), and $\bar{\mathcal{C}}$ is the set of other intermediate codes (i.e., non-leaf nodes) representing more general concepts.*

For simplicity, we define a function $\text{ancestor}(\mathbf{c}, l) : \{0, 1\}^{|\mathcal{C}|} \times \mathbb{Z} \rightarrow \{0, 1\}^{|\bar{\mathcal{C}}|}$, which maps a given medical code $\mathbf{c} \in \{0, 1\}^{|\mathcal{C}|}$ to its l -th level ancestor code (i.e., category). For example, in Fig. 1, the root node is the 0-th level ancestor code of all leaf codes.

Definition 3 (Medical Code Embedding) *To fully utilize the code semantic information, it is a common practice to convert the medical code from one-hot vector $\mathbf{c} \in \{0, 1\}^{|\mathcal{C}|}$ to a dense embedding vector $\mathbf{e} \in \mathbb{R}^d$ (Choi et al., 2016a; Li et al., 2020), where d is the embedding dimensionality. This can be done via an embedding matrix $\mathbf{E} \in \mathbb{R}^{|\mathcal{C}| \times d}$, where each row corresponds to the embedding for a medical code. The embedding can be computed as $\mathbf{e} = \mathbf{E}^\top \mathbf{c}$.*

We denote the embedding matrices for source and target datasets as \mathbf{E}_S and \mathbf{E}_T , respectively. The source embedding \mathbf{E}_S is provided with the trained backbone model as the input. And the target embedding \mathbf{E}_T will be learned using the target dataset. In this work, to deploy the backbone model, we will learn a mapping from the source to the target embedding space.

Definition 4 (Code Embedding Mapping) *We define the mapping from the embedding space of one medical coding system to another as $\phi(\mathbf{E}) : \mathbb{R}^d \rightarrow \mathbb{R}^d$.*

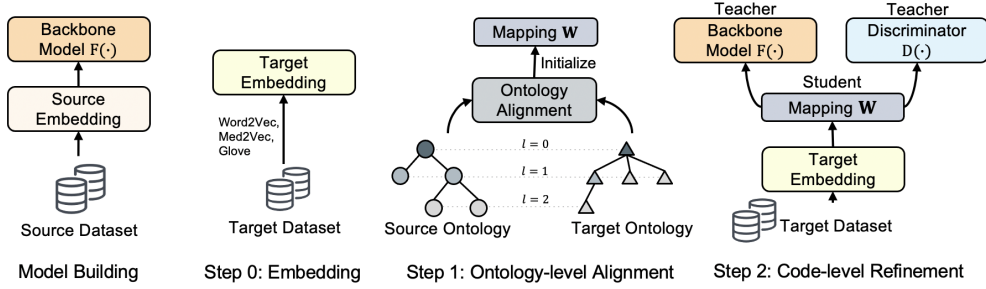


Figure 1: An overview of **AutoMap**. **AutoMap** supports model deployment by automatically mapping the medical code embeddings across different coding systems in a coarse-to-fine manner: (0) Embedding that initializes the target code embedding matrix; (1) Ontology-level Alignment that leverages the ontology structure to learn the coarse ontology mapping; (2) Code-level Refinement that refines the mapping at the fine-grained code level for the downstream task with a teacher-student framework.

We will learn the embedding mapping $\phi(\cdot)$ that maps the target embedding to the source via $\phi(\mathbf{E}_T)$.

Definition 5 (Backbone Deep Learning Model)

The backbone deep learning model $F(\cdot)$ takes EHR sequences and the corresponding medical code embeddings as the input and then outputs the prediction: $\hat{\mathbf{y}} = F([v^{(i)}]_{i=1}^n, \phi(\mathbf{E}))$, where $\hat{\mathbf{y}}$ is the corresponding predictions for label \mathbf{y} . The backbone model $F(\cdot)$ is pre-trained on source dataset $*S$ and deployed on target dataset $*T$ with a different coding system. Note that the embedding mapping $\phi(\cdot)$ degenerates to the identity function if the backbone model $F(\cdot)$ is trained and deployed on the same coding system.

We evaluate **AutoMap** with different backbone models ranging from classic MLP and RNN to more recent GNN and attention-based models on the following tasks.

Task 1 (Mortality Prediction) Given a patient’s EHR data $[v^{(i)}]_{i=1}^n$, we aim to predict mortality $y_M \in \{0, 1\}$ using the backbone model $F_M(\cdot)$. Formally, $\hat{y}_M = F_M([v^{(i)}]_{i=1}^n, \phi(\mathbf{E}))$, where $\hat{y}_M \in \{0, 1\}$.

Task 2 (Length-of-Stay Estimation) Given a patient’s EHR data $[v^{(i)}]_{i=1}^n$, we aim to predict the patient’s length of stay $\mathbf{y}_L \in \mathbb{R}^n$ using a backbone model $F_R(\cdot)$. We follow previous works (Harutyunyan et al., 2019) to categorize label \mathbf{y}_L into four classes $\{0, 1, 2, 3\}$, i.e., less than 1 day (class 0), 1 to 7 days (class 1), 7 to 14 days (class 2), and more than 14 days (class 3). In this way, we frame

length-of-stay estimation as a multi-class classification task. Formally, $\hat{\mathbf{y}}_L = F_R([v^{(i)}]_{i=1}^n, \phi(\mathbf{E}))$, where $\hat{\mathbf{y}}_L \in \{0, 1, 2, 3\}^n$.

We note that **AutoMap** is general and can support other prediction tasks as well.

Problem 1 (Predictive Model Deployment)

Given a backbone model $F(\cdot)$ and source code embedding matrix \mathbf{E}_S , a mostly unlabeled target dataset $*T$ in a different coding system, and the medical ontologies $\mathcal{O}_S, \mathcal{O}_T$ for both coding systems, the goal is to optimize the mapping $\phi(\cdot)$ on the target dataset $*T$, as given by Eq. (1),

$$\arg \min_{\phi(\cdot)} \mathcal{L}(F(\cdot), \mathbf{E}_S, *T, \mathcal{O}_S, \mathcal{O}_T, \phi(\cdot)), \quad (1)$$

where $\mathcal{L}(\cdot)$ denotes the designated loss function. The prediction on the target dataset can be obtained via $F(V_T, \phi(\mathbf{E}_T))$, where V_T is a sequence of visits from the target dataset $*T$, and $\phi(\mathbf{E}_T)$ is the transformed target embeddings.

In our setting, we can only access the source code embedding \mathbf{E}_S and ontology \mathcal{O}_S instead of the source data $*S$. This is more realistic in deployment setting since the source data often cannot be shared due to legal and privacy concern. In contrast, the source embedding matrix \mathbf{E}_S can be more easily provided along with the backbone model $F(\cdot)$, and the code ontologies are usually publicly accessible. We also assume that the target dataset $*T$ is mostly unlabeled, since the target site may often be some small hospital.

3.2. The AutoMap Method

We propose AutoMap for automatic code mapping across different hospitals EHR systems. The mapping will be done in a coarse-to-fine manner, enabled by the adaptation process shown in Fig. 1. Embedding (step 0) first initializes the target code embedding matrix \mathbf{E}_T . Ontology-level alignment (step 1) then derives the initial coarse mapping $\phi(\cdot)$ via iterative self-supervised learning. Code-level refinement (step 2) further fine-tunes the mapping $\phi(\cdot)$ at the code level using a teacher-student framework.

3.2.1. STEP 0: EMBEDDING.

As mentioned in Def. 3, we first convert the target medical codes from one-hot vector $\mathbf{c}_T \in \{0, 1\}^{|\mathcal{C}|}$ to a corresponding dense embedding vector $\mathbf{e}_T \in \mathbb{R}^d$. We use GloVe (Pennington et al., 2014) to learn the target code embedding matrix \mathbf{E}_T via a global co-occurrence matrix of medical codes. Other unsupervised learning algorithms such as Med2Vec (Choi et al., 2016c) and Word2Vec (Mikolov et al., 2013a) can also be used. We employ GloVe because of its computational efficiency.

Code embeddings can also be computed based on code text descriptions. However, the text descriptions may bring in additional noise, which may confuse the mapping. Moreover, under the extreme case where the model is trained and deployed on two completely different coding systems (e.g., from diagnosis codes to medication codes), the text descriptions may not help since the descriptions are too different. On the contrary, we show empirically that AutoMap can still adapt to this extreme case.

After that, we parameterize $\phi(\cdot)$ by a mapping matrix $\mathbf{W} \in \mathbb{R}^{d \times d}$. The mapping matrix \mathbf{W} can be used to transform the target code embedding via $\mathbf{E}_T \mathbf{W}$.

3.2.2. STEP 1: ONTOLOGY-LEVEL ALIGNMENT.

In this step, we will first learn a coarse mapping \mathbf{W} at the ontology level. This first step is essential because direct code level mapping is difficult and unnecessary: (1) It is difficult due to the large number of medical codes; (2) It is also unnecessary since many codes have similar clinical meanings. Therefore, we follow a common practice to first group similar codes using code ontology (Choi et al., 2016c,a; Shang et al., 2019) and learn the mapping on groups instead of leaf-level codes. For example, ICD-9 code 438.11 “late effects of cerebrovascular disease,

aphasia” corresponds to five ICD-10 codes (I69.020, I69.120, I69.220, I69.320, I69.920). While it is hard to directly align the ICD-9 code to each of these five ICD-10 codes, we can first coarsely map the ICD-9 code to I00-I99 “diseases of the circulatory system”, and then gradually refine the mapping to I60-I99 “cerebrovascular diseases”, I69 “cerebrovascular diseases”, and eventually the five-leaf codes. By leveraging the medical ontology, we can use more general medical concepts as “anchor points” to better align two coding systems.

Next, we introduce the building blocks of the iterative self-supervised learning (i.e., ontology grouping, unsupervised seed induction, Procrustes refinement), and then present the ontology-level alignment algorithm.

Ontology Grouping. At a given hierarchy level l , we group the codes according to their l -th level ontology categories. Specifically, the i -th group $\mathcal{G}_i^{(l)}$ consists of all the leaf medical codes whose l -th level category is \mathbf{c}_i , as in Eq. (2),

$$\mathcal{G}_i^{(l)} = \{\mathbf{c}_j \mid \text{ancestor}(\mathbf{c}_j, l) = \mathbf{c}_i, \mathbf{c}_j \in \mathcal{C}\}, \quad (2)$$

where $\mathbf{c}_i \in \bar{\mathcal{C}}$ is the corresponding l -th level category code. We will drop the superscript $^{(l)}$ whenever it is unambiguous.

To obtain the group embedding \mathbf{g}_i , we first calculate the mean group embedding $\bar{\mathbf{g}}_i$ by averaging all the code embeddings in that group, as in Eq. (3a); then, we represent the group embedding as the closest code embedding, as in Eq. (3b),

$$\bar{\mathbf{g}}_i = \text{mean}\{\mathbf{e}_j \mid \mathbf{c}_j \in \mathcal{G}_i\}, \quad (3a)$$

$$\mathbf{g}_i = \underset{\mathbf{e}_j}{\text{argmin}}\{\mathbf{e}_j \bar{\mathbf{g}}_i^\top \mid \mathbf{c}_j \in \mathcal{C}\}, \quad (3b)$$

where \mathbf{e}_j is the embedding vector for the code \mathbf{c}_j , and $\mathbf{e}_j \bar{\mathbf{g}}_i^\top \in \mathbb{R}$ calculates the distance between the code \mathbf{c}_j and the mean group embedding $\bar{\mathbf{g}}_i$. Intuitively, \mathbf{g}_i can be viewed as the “median” group embedding. We select the top- k groups based on the group size, since we want to first learn a coarse mapping, while including too many groups may introduce too much granular information. As a result, we have $\mathbf{G}_T, \mathbf{G}_S \in \mathbb{R}^{k \times d}$ for target and source groups, where each row corresponds to an embedding vector for a particular group. We present with the same k to reduce clutter, though it can be different for source and target groups.

We note that when the ontology is not available, AutoMap can still apply by using a clustering algorithm (e.g., k-Means) to group the medical codes.

Specifically, we provide additional experiments on this setting in Appx. H.2.

Unsupervised Seed Induction. Given the l -th level source and target coding groups \mathbf{G}_S and \mathbf{G}_T , we can initialize a coarse alignment in a fully unsupervised way. More specifically, we first calculate the similarity matrices, as in Eq. (4),

$$\mathbf{M}_T = \mathbf{G}_T \mathbf{G}_T^\top; \mathbf{M}_S = \mathbf{G}_S \mathbf{G}_S^\top, \quad (4)$$

where $\mathbf{M}_T, \mathbf{M}_S \in \mathbb{R}^{k \times k}$. Each row in the similarity matrices $\mathbf{M}_T, \mathbf{M}_S$ represents the similarities of the corresponding group to all the other groups. Under the ideal case where the embedding spaces between different coding systems are isometric¹, one can permute the rows and columns of \mathbf{M}_T to obtain \mathbf{M}_S . We introduce the following heuristics to find the optimal permutation (i.e., a mapping dictionary) of this NP-hard problem (Karp, 1972). We perform row-wise sort on \mathbf{M}_T and \mathbf{M}_S (i.e., elements in each row are sorted based only on the order in that particular row), as in Eq. (5a). Under the isometric assumption, codes with the same meaning will have exactly the same row vector in $\tilde{\mathbf{M}}_T$ and $\tilde{\mathbf{M}}_S$, suggesting that we can find the mapping dictionary $\mathbf{D} \in \mathbb{R}^{k \times k}$ via nearest neighbor search over row vectors in $\tilde{\mathbf{M}}_T$, as shown in Eq. (5b),

$$\tilde{\mathbf{M}}_T = \text{sorted}(\mathbf{M}_T); \tilde{\mathbf{M}}_S = \text{sorted}(\mathbf{M}_S), \quad (5a)$$

$$\mathbf{D}[i, j] = \begin{cases} 1, & \text{if } j = \text{argmax}((\tilde{\mathbf{M}}_T \cdot \tilde{\mathbf{M}}_S^\top)[i, :]) \\ 0, & \text{otherwise,} \end{cases} \quad (5b)$$

where \cdot denotes matrix multiplication.

Procrustes Optimization. At a given hierarchy level l , we optimize the inducted mapping dictionary \mathbf{D} by iterating the following two steps.

1. The mapping $\mathbf{W} \in \mathbb{R}^{d \times d}$ is obtained by maximizing the similarities for the current dictionary \mathbf{D} as given by Eq. (6a). This optimization problem is known as the Procrustes problem (Schönemann, 1966) and has a closed form

solution, as in Eq. (6b),

$$\underset{\mathbf{W}}{\text{argmin}} \|\mathbf{D} \odot (\underbrace{\mathbf{G}_T \mathbf{W} \mathbf{G}_S^\top}_{\text{transformed target embedding}})\|_1, \quad (6a)$$

$$\mathbf{W} = \mathbf{U} \mathbf{V}^\top, \text{ where } \mathbf{U} \mathbf{\Sigma} \mathbf{V}^\top = \text{SVD}(\mathbf{G}_T^\top \mathbf{D} \mathbf{G}_S), \quad (6b)$$

where \odot denotes Hadamard product, and SVD denotes Singular Value Decomposition (Klema and Laub, 1980).

2. A new dictionary \mathbf{D} is induced, as in Eq. (7),

$$\mathbf{D}[i, j] = \begin{cases} 1, & \text{if } j = \text{argmax}((\mathbf{G}_T \mathbf{W} \mathbf{G}_S^\top)[i, :]) \\ 0, & \text{otherwise.} \end{cases} \quad (7)$$

Iterative Self-supervised Learning. We now introduce the self-supervised learning strategy, which maps the two coding systems at multiple resolutions iteratively. Starting from a coarse hierarchy level l , we obtain the l -th level medical coding groups \mathbf{G}_S and \mathbf{G}_T with Eq. (2, 3). Then we induct the l -th level seed mapping dictionary $\mathbf{D}^{(l)}$ with Eq. (4, 5). Next, we merge the current and previous level mapping dictionaries, as $\mathbf{D}^{(l)} = \mathbf{D}^{(l)} + \mathbf{D}^{(l-1)}$. Lastly, we optimize the merged mapping dictionary $\mathbf{D}^{(l)}$ using Eq. (6, 7). We gradually increase l (going down in the ontology) during iterative self-supervised learning until we reach the leaf level to learn the mapping at multiple resolutions. We note that source and target codes can use different grouping level l . We present with the same l to reduce clutter.

In this way, we learn a coarse mapping matrix \mathbf{W} between two medical coding systems at the ontology level. This step is inspired by Artetxe et al. (2018). However, instead of directly mapping medical codes, AutoMap leverages the ontology structure and iteratively maps medical coding groups in a coarse-to-fine manner, allowing AutoMap to better align coding systems with different granularities.

3.2.3. STEP 2: CODE-LEVEL REFINEMENT.

While we have performed step 1 (ontology-level alignment) to initialize the mapping, the mapping is still too coarse and need further refining. Moreover, there is no guarantee of the performance for the downstream tasks (i.e., mortality prediction and length-of-stay estimation). Thus, it is preferred to further fine-tune the mapping at the code level for downstream tasks.

1. In practice, the isometry requirement will not hold exactly, but it can be assumed to hold approximately, or the problem of mapping two code embedding spaces without supervision would be impossible.

To do this, we propose a teacher-student framework, where the discriminator $D(\cdot)$ (teacher A) refines the mapping matrix \mathbf{W} (student) via adversarial learning; and the backbone model $F(\cdot)$ (teacher B) optimizes the mapping matrix \mathbf{W} (student) based on the final prediction task. Below we describe the framework in detail.

Teacher A: Discriminator. We leverage the adversarial learning framework by introducing a discriminator $D(\cdot)$, parameterized by a multi-layer neural network. Specifically, the discriminator $D(\cdot)$ tries to classify whether the embeddings are from the target (label 0) or source (label 1) embedding distributions. Formally, discriminator $D(\cdot)$ aims at minimizing the discriminator adversarial loss, as in Eq. (8),

$$\mathcal{L}_D = -\log(D(\mathbf{e}_S)) - \log(D(1 - \mathbf{e}_T \mathbf{W})), \quad (8)$$

where \mathbf{e}_S (\mathbf{e}_T) represents the source (target) code embedding sampled randomly from the code embedding matrix \mathbf{E}_S (\mathbf{E}_T), and \mathbf{W} maps the target embedding to the source embedding space via $\mathbf{e}_T \mathbf{W}$.

The mapping matrix \mathbf{W} acts as the generator and tries to deceive the discriminator $D(\cdot)$. Formally, we try to minimize the generator adversarial loss, as in Eq. 9,

$$\mathcal{L}_G = -\log(D(\mathbf{e}_T \mathbf{W})). \quad (9)$$

Theoretically, the discriminator $D(\cdot)$ and mapping matrix \mathbf{W} learn to align two coding systems as an adversarial game, which is essentially minimizing the following Jensen-Shannon divergence (JSD) (Goodfellow et al., 2014), as shown in Eq. (10),

$$\text{JSD}(p(\mathbf{e}_S) \| p(\mathbf{e}_T \mathbf{W})). \quad (10)$$

The definition of JSD can be found in Appx. C. Note that since the minimization happens at the distribution level, we do not require code mapping pairs to supervise training.

Teacher B: Backbone. Here, the backbone model $F(\cdot)$ is leveraged to optimize the ultimate prediction performance based on the transformed target code embeddings. Formally, we aim at minimizing the following classification loss

$$\mathcal{L}_{\text{cls}}(F([v^{(i)}]_{i=1}^n, \mathbf{E}_T \mathbf{W}), \mathbf{y}_T), \quad (11)$$

where the transformed target code embeddings $\mathbf{E}_T \mathbf{W}$ are used to encode patient visits $[v^{(i)}]_{i=1}^n$.

In summary, the mapping matrix \mathbf{W} is fine-tuned by minimizing the combined loss

$$\mathcal{L}_W = \mathcal{L}_{\text{cls}} + \alpha \mathcal{L}_G, \quad (12)$$

where α is a hyper-parameter to balance the two teachers. The pseudo-code of AutoMap can be found in Appx. D.

3.2.4. REMARKS.

Step 2 (code-level refinement) assumes a white-box backbone model $F(\cdot)$. If $F(\cdot)$ is a blackbox model, we will perform step 1 (ontology-level alignment).

4. Experiment

We deploy AutoMap with several backbone deep learning models and test on two real-world EHR datasets to answer the following questions:

1. Can AutoMap deploy backbone deep learning models to target hospitals with limited labeled data?
2. Can AutoMap learn accurate mapping across different coding systems?
3. Can AutoMap adapt to target hospitals with completely different coding systems?
4. Can AutoMap adapt to target hospitals from completely different regions?

4.1. Experimental Setting

Data. We evaluate the performance of AutoMap extensively with two publicly accessible datasets: eICU (Pollard et al., 2018) and MIMIC-III (Johnson et al., 2016). eICU (Pollard et al., 2018) is a multi-center database with intensive care unit (ICU) records for over 200K admissions to over 200 hospitals across the United States. MIMIC-III (Johnson et al., 2016) is a single-center database containing 53K ICU records from Beth Israel Deaconess Medical Center.

For Q1 (limited labeled data) and Q2 (mapping accuracy), we use eICU (Pollard et al., 2018) to evaluate the model performance across ICD-9 and ICD-10 codes. For Q3 (different coding systems), we evaluate this scenario with MIMIC-III (Johnson et al., 2016). The backbone model is trained on diagnosis codes (ICD-9) and then deployed on medication codes (NDC). For Q4 (different hospitals), we use the multi-center database eICU (Pollard

et al., 2018). Following previous work (Zhang et al., 2021b), we train the backbone model in hospitals from Midwest region and deploy it to hospitals from South region. Detailed setting and statistics can be found in Appx. E.

Baselines. Next, we present all the baselines.

- **Direct Training:** Directly train a new model on the target dataset.
- **Transfer Learning:** Swap the embedding matrix and fine-tune the new embedding with the backbone model.
- **Mapping Tools:** Map target medical codes to the source using existing code mapping tools.
- **MUSE (Conneau et al., 2018):** Learn the mapping by aligning the target and source embedding distributions via adversarial learning.
- **VecMap (Artetxe et al., 2018):** Learn the mapping via iterative self-supervised learning based on the code-level structure similarity.

Lastly, we conduct an ablation study of our `AutoMap`.

- **Step 1 Only:** We only perform step 1 (ontology-level alignment) to learn the mapping matrix \mathbf{W} . Then we directly use the transformed target embedding for the downstream task. This is to evaluate the contribution of the ontology mapping.
- **Step 1 Only + Random Ontology:** We only perform step 1 (ontology-level alignment) but with a randomly generated ontology. This is to evaluate the contribution of leveraging medical ontology.
- **Step 2 Only:** We randomly initialize the mapping matrix \mathbf{W} and then only perform step 2 code-level refinement. This is to evaluate the contribution of the teacher-student framework.

Backbone Models. As `AutoMap` is a general framework that can apply to different backbone models, we incorporate `AutoMap` with the following backbone deep learning models:

- **MLP:** Learn the visit representation using a simple feed-forward neural network.
- **RNN:** Learn the visit representation using a simple recurrent neural network.

- **RETAIN (Choi et al., 2016a):** A two-level neural attention model which can detect influential past visits and significant clinical variable within those visits.
- **GCT (Choi et al., 2020):** A graph convolutional transformer which jointly learns the hidden structure of EHR while performing supervised prediction tasks on EHR data.
- **BEHRT (Li et al., 2020):** A deep neural sequence transduction model based on BERT (Devlin et al., 2019), which performs self-attention mechanism (Vaswani et al., 2017) on the sequence of visits.

4.2. Q1: Target Data with Limited Labels

We first evaluate `AutoMap` in a common setting where the target site has limited labeled data (100 patients). Results can be found in in Tab. 1. For reference, we also report the performance of the model trained with the fully-labeled target data, as “*Full-Label*” in the table. This can be viewed as an “upper bound” of the model performance. Due to the limited space, we only report AUC-PR for mortality and F1 for length-of-stay here. Additional results can be found in Appx. H.1. Descriptions of the metrics can be found in Appx G.

As shown in Tab. 1, first, we find that the two simple baselines: direct training and transfer learning methods do not work very well. In most cases, they are much worse compared to the full-label performance. This is expected as the amount of labeled data is insufficient to train or fine-tune the backbone models. Next, code-level mapping methods MUSE (Conneau et al., 2018) and VecMap (Artetxe et al., 2018) achieve some improvements, but they are not stable. In some cases, they perform even worse than the two simple baselines. This may be because ICD-9 and ICD-10 have different degrees of specificity (e.g., 10K codes in ICD-9 v.s. 68K codes in ICD-10), and directly mapping them at code level does not work very well. Finally, we observe that `AutoMap` achieves significant improvement over the baseline and can match the full-label performance in most cases. Specifically, `AutoMap` achieves up to 8.7% relative improvement on AUC-PR score for mortality prediction; for length-of-stay estimation, `AutoMap` achieves up to and 3.7% relative improvement on F1 score. This demonstrates the effectiveness of coarse-to-fine mapping and the versatility of `AutoMap`.

Backbone	Method	Mortality AUC-PR	Length-of-Stay F1
MLP	<i>Full-Label</i>	<i>0.2819 ± 0.0317</i>	<i>0.5033 ± 0.0169</i>
	Direct Training	0.2524 ± 0.0285	0.2835 ± 0.0147
	Transfer Learning	0.2551 ± 0.0287	0.4584 ± 0.0179
	MUSE	0.2506 ± 0.0279	0.4905 ± 0.0172
	VecMap	0.2820 ± 0.0315	0.4947 ± 0.0171
	AutoMap	0.2934 ± 0.0324*	0.4952 ± 0.0168
RNN	<i>Full-Label</i>	<i>0.2818 ± 0.0319</i>	<i>0.5030 ± 0.0167</i>
	Direct Training	0.2074 ± 0.0236	0.1222 ± 0.0089
	Transfer Learning	0.2536 ± 0.0286	0.4662 ± 0.0176
	MUSE	0.2455 ± 0.0275	0.4933 ± 0.0169
	VecMap	0.2780 ± 0.0311	0.5019 ± 0.0168
	AutoMap	0.2875 ± 0.0319*	0.4996 ± 0.0163
RETAIN	<i>Full-Label</i>	<i>0.2648 ± 0.0302</i>	<i>0.4447 ± 0.0183</i>
	Direct Training	0.2031 ± 0.0228	0.1222 ± 0.0089
	Transfer Learning	0.2269 ± 0.0262	0.4455 ± 0.0179
	MUSE	0.2374 ± 0.0283	0.4217 ± 0.0185
	VecMap	0.2744 ± 0.0305	0.4264 ± 0.0184
	AutoMap	0.2835 ± 0.0313*	0.4779 ± 0.0167*
GCT	<i>Full-Label</i>	<i>0.2814 ± 0.0323</i>	<i>0.4986 ± 0.0163</i>
	Direct Training	0.1836 ± 0.0189	0.2680 ± 0.0158
	Transfer Learning	0.2103 ± 0.0222	0.4748 ± 0.0162
	MUSE	0.2242 ± 0.0250	0.4866 ± 0.0159
	VecMap	0.2491 ± 0.0264	0.4863 ± 0.0162
	AutoMap	0.2707 ± 0.0294*	0.4940 ± 0.0164*
BEHRT	<i>Full-Label</i>	<i>0.2652 ± 0.0275</i>	<i>0.3657 ± 0.0176</i>
	Direct Training	0.1740 ± 0.0163	0.3063 ± 0.0163
	Transfer Learning	0.2320 ± 0.0249	0.3291 ± 0.0178
	MUSE	0.2155 ± 0.0222	0.3493 ± 0.0178
	VecMap	0.2786 ± 0.0292	0.3612 ± 0.0179
	AutoMap	0.2712 ± 0.0280	0.3744 ± 0.0182*

Table 1: Results with limited labeled data (100 patients) in the target site. Dataset is eICU (Pollard et al., 2018). The average scores of two mapping directions between ICD-9 and ICD-10 codes are reported. ± denotes standard deviations. * indicates that **AutoMap** achieves significant improvement over the best baseline method (i.e., p-value is smaller than 0.05). Experiment results show that **AutoMap** can adapt different backbone models to the target site with limited labeled data.

4.3. Q2: Mapping Accuracy

We then evaluate the accuracy of the learnt mapping. The ICD code mapping in the eICU (Pollard et al., 2018) dataset is used as the ground truth. Due to the limited space, for the rest of the experiments, we only report results with BEHRT (Li et al., 2020) using 100 labeled patients in the target data.

As shown in Tab. 2, VecMap (Artetxe et al., 2018) and **AutoMap** achieve much better performance than MUSE (Conneau et al., 2018). This supports the isometric assumption used in both methods. Further, **AutoMap** achieves the best results with statis-

Method	Similarity	Hit@10
MUSE	0.1633 ± 0.0110	0.0600 ± 0.0113
VecMap	0.4612 ± 0.0980	0.5974 ± 0.1841
AutoMap	0.4992 ± 0.0070*	0.6657 ± 0.0187*

Table 2: Accuracy of mapping for diagnosis codes (ICD-9 and ICD-10). Dataset is eICU (Pollard et al., 2018). The average scores of two mapping directions are reported. Experiment results show that **AutoMap** can learn accurate mapping across medical coding systems.

tical significance. This demonstrates that the proposed coarse-to-fine mapping can better map coding systems with different granularities.

4.4. Q3: Completely Different Codes

Method	Mortality AUC-PR	Length-of-Stay F1
<i>Full-Label</i>	<i>0.7149 ± 0.0227</i>	<i>0.3057 ± 0.0173</i>
Direct Training	0.4701 ± 0.0236	0.3158 ± 0.0174
Transfer Learning	0.5642 ± 0.0255	0.2999 ± 0.0171
MUSE	0.4905 ± 0.0241	0.3022 ± 0.0171
VecMap	0.3553 ± 0.0173	0.3014 ± 0.0171
AutoMap	0.5902 ± 0.0252*	0.3022 ± 0.0171

Table 3: Results for the scenario where the backbone model is trained on diagnosis code (ICD-9) and deployed on medication codes (NDC). Dataset is MIMIC-III (Johnson et al., 2016). Experiment results show that **AutoMap** can adapt to target data coded in a completely different system.

We next evaluate **AutoMap** on the challenging case where we train the backbone model on diagnosis code (ICD-9) and deploy it on medication codes (NDC). Results can be found in in Tab. 3.

First, we note that since these two coding systems are so different, no existing mapping tools is available. For mortality prediction, as shown in Tab. 3, the code-level mapping methods perform even worse than direct training and transfer learning. This may be due to the large gap between these two coding systems. On the contrary, **AutoMap** can still give accept-

able results, outperforming all baseline methods with 4.6% – 66.1% statistically significant improvements. This shows the superiority of **AutoMap**’s coarse-to-fine mapping strategy. For the length-of-stay estimation task, all five methods perform pretty similar to full-label performance. This may indicate that medication codes are not so informational for length-of-stay estimation.

4.5. Q4: Completely Different Hospitals

Method	Mortality AUC-PR	Length-of-Stay F1
<i>Full-Label</i>	0.2578 ± 0.0300	0.4560 ± 0.0158
Direct Training	0.1434 ± 0.0154	0.4334 ± 0.0164
Transfer Learning	0.1860 ± 0.0214	0.3924 ± 0.0158
MUSE	0.1314 ± 0.0150	0.3988 ± 0.0165
VecMap	0.1305 ± 0.0163	0.3801 ± 0.0167
AutoMap	$0.1990 \pm 0.022^*$	0.4290 ± 0.0157

Table 4: Results for the scenario where the backbone model is trained and deployed in hospitals from different regions. Dataset is eICU (Pollard et al., 2018). Experiment results show that **AutoMap** can adapt to target hospitals from a completely region.

We further challenge **AutoMap** under the scenario where we train the backbone model in hospitals from Midwest region (with ICD-9 code) and deploy it in hospitals from South region (with ICD-10 code). Results can be found in in Tab. 4.

For mortality prediction, mapping based methods (MUSE (Conneau et al., 2018) and VecMap (Artetxe et al., 2018)) achieve the worst results. This is expected as methods from cross-lingual word mapping do not consider the domain gap between different regions. This also explains why transfer learning perform slightly better (as its training scheme can accommodate some domain gap). Benefit from the refinement step, **AutoMap** achieves the best result with 7.0% – 52.5% statistically significant relative improvements. This shows that **AutoMap** can adapt to hospitals from different regions. For length-of-stay estimation, all pre-training based methods perform worse than direct training. This may indicate that different hospitals have different decision rules on ICU length-of-stay. As a result, transferring knowledge from other hospitals may not help. Despite this, **AutoMap**

still achieves the best results among all pre-training based methods.

4.6. Ablation study

Method	Mortality AUC-PR	Length-of-Stay F1
Step 1 Only	0.2680 ± 0.0275	0.3623 ± 0.0181
Step 1 Only + R.O.	0.2054 ± 0.0215	0.3631 ± 0.0179
Step 2 Only	0.2038 ± 0.0213	0.3306 ± 0.0181
AutoMap	$0.2712 \pm 0.0280^*$	$0.3744 \pm 0.0182^*$

Table 5: Ablation study. Dataset is eICU (Pollard et al., 2018). The average scores of two mapping directions between ICD-9 and ICD-10 codes are reported. R.O. denotes random ontology. Experiment results demonstrate the importance of **AutoMap**’s 2-step coarse-to-fine mapping.

Finally, we compare **AutoMap** with three ablated versions. As shown in Tab. 5, only performing step 2 (code-level refinement) gives the worst results. This is reasonable as the model will easily over-fit the target data with limited labels. Also, since the mapping matrix \mathbf{W} is randomly generated, the adversarial learning module will even harm the downstream tasks. Next, we can see that performing step 1 (ontology-level alignment) only gives better results. This indicates that step 1 contributes most to **AutoMap**’s improvements. This may because the isometric assumption and medical ontology can act as a strong prior to guide the model learning process. This point can also be supported by the performance with randomly-generated ontology. Lastly, **AutoMap** achieves the best results. This shows the importance of refining the mapping at code-level after the coarse ontology alignment.

5. Conclusion

We propose **AutoMap**, an automatic for automatic medical code mapping across different hospitals EHR systems. **AutoMap** is enabled by the following process: (0) Embedding: We construct target embeddings from a target dataset. (1) Ontology-level Alignment: We leverage the ontology structure to learn a coarse ontology-level mapping; (2) Code-level Refinement: We further refine the mapping at the fine-grained

code level for the downstream task. Benefit from this coarse-to-fine mapping, `AutoMap` can better align coding systems at different granularities. We evaluate `AutoMap` extensively using different backbone models with two real-world EHR datasets. Experimental results show that `AutoMap` outperforms existing solutions on multiple prediction tasks when mapping solutions exist and provides a mapping strategy when conventional solutions do not exist. To our best knowledge, `AutoMap` is the first work towards code-agnostic deep learning deployment in the healthcare domain without relying on existing code mapping tools.

Institutional Review Board (IRB)

This research does not require IRB approval.

References

- Mikel Artetxe, Gorka Labaka, and Eneko Agirre. Learning bilingual word embeddings with (almost) no bilingual data. In *Proceedings of the 55th Annual Meeting of the Association for Computational Linguistics (Volume 1: Long Papers)*, pages 451–462, Vancouver, Canada, July 2017. Association for Computational Linguistics. doi: 10.18653/v1/P17-1042. URL <https://www.aclweb.org/anthology/P17-1042>.
- Mikel Artetxe, Gorka Labaka, and Eneko Agirre. A robust self-learning method for fully unsupervised cross-lingual mappings of word embeddings. In *Proceedings of the 56th Annual Meeting of the Association for Computational Linguistics (Volume 1: Long Papers)*, pages 789–798, Melbourne, Australia, July 2018. Association for Computational Linguistics. doi: 10.18653/v1/P18-1073. URL <https://www.aclweb.org/anthology/P18-1073>.
- Inci M. Baytas, Cao Xiao, Xi Zhang, Fei Wang, Anil K. Jain, and Jiayu Zhou. Patient subtyping via time-aware lstm networks. In *Proceedings of the 23rd ACM SIGKDD International Conference on Knowledge Discovery and Data Mining*, KDD '17, page 65–74, New York, NY, USA, 2017. Association for Computing Machinery. ISBN 9781450348874. doi: 10.1145/3097983.3097997. URL <https://doi.org/10.1145/3097983.3097997>.
- Guthrie S. Birkhead, Michael Klompas, and Nirav R. Shah. Uses of electronic health records for public health surveillance to advance public health. *Annual Review of Public Health*, 36(1):345–359, 2015. doi: 10.1146/annurev-publhealth-031914-122747. URL <https://doi.org/10.1146/annurev-publhealth-031914-122747>. PMID: 25581157.
- O. Bodenreider. The Unified Medical Language System (UMLS): integrating biomedical terminology. *Nucleic Acids Res*, 32(Database issue):D267–270, Jan 2004.
- Edward Choi, Mohammad Taha Bahadori, Joshua A. Kulas, Andy Schuetz, Walter F. Stewart, and Jimeng Sun. Retain: An interpretable predictive model for healthcare using reverse time attention mechanism. In *Proceedings of the 30th International Conference on Neural Information Processing Systems*, NIPS'16, page 3512–3520, Red Hook, NY, USA, 2016a. Curran Associates Inc. ISBN 9781510838819.
- Edward Choi, Mohammad Taha Bahadori, Andy Schuetz, Walter F. Stewart, and Jimeng Sun. Doctor ai: Predicting clinical events via recurrent neural networks. In Finale Doshi-Velez, Jim Fackler, David Kale, Byron Wallace, and Jenna Wiens, editors, *Proceedings of the 1st Machine Learning for Healthcare Conference*, volume 56 of *Proceedings of Machine Learning Research*, pages 301–318, Northeastern University, Boston, MA, USA, 18–19 Aug 2016b. PMLR. URL <https://proceedings.mlr.press/v56/Choi16.html>.
- Edward Choi, Mohammad Taha Bahadori, Elizabeth Searles, Catherine Coffey, Michael Thompson, James Bost, Javier Tejedor-Sojo, and Jimeng Sun. Multi-layer representation learning for medical concepts. In *Proceedings of the 22nd ACM SIGKDD International Conference on Knowledge Discovery and Data Mining*, KDD '16, page 1495–1504, New York, NY, USA, 2016c. Association for Computing Machinery. ISBN 9781450342322. doi: 10.1145/2939672.2939823. URL <https://doi.org/10.1145/2939672.2939823>.
- Edward Choi, Mohammad Taha Bahadori, Le Song, Walter F. Stewart, and Jimeng Sun. Gram: Graph-based attention model for healthcare representation learning. In *Proceedings of the 23rd ACM*

- SIGKDD International Conference on Knowledge Discovery and Data Mining*, KDD '17, page 787–795, New York, NY, USA, 2017. Association for Computing Machinery. ISBN 9781450348874. doi: 10.1145/3097983.3098126. URL <https://doi.org/10.1145/3097983.3098126>.
- Edward Choi, Zhen Xu, Yujia Li, Michael Dusenberry, Gerardo Flores, Emily Xue, and Andrew Dai. Learning the graphical structure of electronic health records with graph convolutional transformer. *Proceedings of the AAAI Conference on Artificial Intelligence*, 34:606–613, 04 2020. doi: 10.1609/aaai.v34i01.5400.
- Alexis Conneau, Guillaume Lample, Marc’Aurelio Ranzato, Ludovic Denoyer, and Hervé Jégou. Word translation without parallel data, 2018.
- Jacob Devlin, Ming-Wei Chang, Kenton Lee, and Kristina Toutanova. BERT: Pre-training of deep bidirectional transformers for language understanding. In *Proceedings of the 2019 Conference of the North American Chapter of the Association for Computational Linguistics: Human Language Technologies, Volume 1 (Long and Short Papers)*, pages 4171–4186, Minneapolis, Minnesota, June 2019. Association for Computational Linguistics. doi: 10.18653/v1/N19-1423. URL <https://www.aclweb.org/anthology/N19-1423>.
- Ian J. Goodfellow, Jean Pouget-Abadie, Mehdi Mirza, Bing Xu, David Warde-Farley, Sherjil Ozair, Aaron Courville, and Yoshua Bengio. Generative adversarial networks, 2014.
- Priyanka Gupta, Pankaj Malhotra, Jyoti Narwariya, Lovekesh Vig, and Gautam Shroff. Transfer learning for clinical time series analysis using deep neural networks, 2019.
- Hrayr Harutyunyan, Hrant Khachatrian, David C. Kale, Greg Ver Steeg, and Aram Galstyan. Multitask learning and benchmarking with clinical time series data. *Scientific Data*, 6(1), Jun 2019. ISSN 2052-4463. doi: 10.1038/s41597-019-0103-9. URL <http://dx.doi.org/10.1038/s41597-019-0103-9>.
- G. Hripcsak, J. D. Duke, N. H. Shah, C. G. Reich, V. Huser, M. J. Schuemie, M. A. Suchard, R. W. Park, I. C. Wong, P. R. Rijnbeek, J. van der Lei, N. Pratt, G. N. Norén, Y. C. Li, P. E. Stang, D. Madigan, and P. B. Ryan. Observational Health Data Sciences and Informatics (OHDSI): Opportunities for Observational Researchers. *Stud Health Technol Inform*, 216:574–578, 2015.
- Alistair EW Johnson, Tom J Pollard, Lu Shen, Liwei H Lehman, Mengling Feng, Mohammad Ghassemi, Benjamin Moody, Peter Szolovits, Leo Anthony Celi, and Roger G Mark. Mimic-iii, a freely accessible critical care database. *Scientific data*, 3: 160035, 2016.
- Richard M. Karp. *Reducibility among Combinatorial Problems*, pages 85–103. Springer US, Boston, MA, 1972. ISBN 978-1-4684-2001-2. doi: 10.1007/978-1-4684-2001-2_9. URL https://doi.org/10.1007/978-1-4684-2001-2_9.
- V. Klementia and A. Laub. The singular value decomposition: Its computation and some applications. *IEEE Transactions on Automatic Control*, 25(2): 164–176, 1980. doi: 10.1109/TAC.1980.1102314.
- Yikuan Li, Shishir Rao, José Roberto Ayala Solares, Abdelaali Hassaine, Rema Ramakrishnan, Dexter Canoy, Yajie Zhu, Kazem Rahimi, and Gholamreza Salimi-Khorshidi. BEHRT: Transformer for Electronic Health Records. *Scientific Reports*, 10 (1):7155, December 2020. ISSN 2045-2322. doi: 10.1038/s41598-020-62922-y. URL <http://www.nature.com/articles/s41598-020-62922-y>.
- Junyu Luo, Muchao Ye, Cao Xiao, and Fenglong Ma. *HiTANet: Hierarchical Time-Aware Attention Networks for Risk Prediction on Electronic Health Records*, page 647–656. Association for Computing Machinery, New York, NY, USA, 2020. ISBN 9781450379984. URL <https://doi.org/10.1145/3394486.3403107>.
- Fenglong Ma, Radha Chitta, Jing Zhou, Quanzeng You, Tong Sun, and Jing Gao. Dipole: Diagnosis prediction in healthcare via attention-based bidirectional recurrent neural networks. In *Proceedings of the 23rd ACM SIGKDD International Conference on Knowledge Discovery and Data Mining*, KDD '17, page 1903–1911, New York, NY, USA, 2017. Association for Computing Machinery. ISBN 9781450348874. doi: 10.1145/3097983.3098088. URL <https://doi.org/10.1145/3097983.3098088>.
- Liantao Ma, Junyi Gao, Yasha Wang, Chaohe Zhang, Jiangtao Wang, Wenjie Ruan, Wen Tang, Xin

- Gao, and Xinyu Ma. Adacare: Explainable clinical health status representation learning via scale-adaptive feature extraction and recalibration. In *The Thirty-Fourth AAAI Conference on Artificial Intelligence, AAAI 2020, The Thirty-Second Innovative Applications of Artificial Intelligence Conference, IAAI 2020, The Tenth AAAI Symposium on Educational Advances in Artificial Intelligence, EAAI 2020, New York, NY, USA, February 7-12, 2020*, pages 825–832. AAAI Press, 2020a. URL <https://aaai.org/ojs/index.php/AAAI/article/view/5427>.
- Liantao Ma, Xinyu Ma, Junyi Gao, Chaohe Zhang, Zhihao Yu, Xianfeng Jiao, Wenjie Ruan, Yasha Wang, Wen Tang, and Jiangtao Wang. Covid-care: Transferring knowledge from existing emr to emerging epidemic for interpretable prognosis, 2020b.
- Liantao Ma, Chaohe Zhang, Yasha Wang, Wenjie Ruan, Jiangtao Wang, Wen Tang, Xinyu Ma, Xin Gao, and Junyi Gao. Concare: Personalized clinical feature embedding via capturing the healthcare context. *Proceedings of the AAAI Conference on Artificial Intelligence*, 34(01): 833–840, Apr. 2020c. doi: 10.1609/aaai.v34i01.5428. URL <https://ojs.aaai.org/index.php/AAAI/article/view/5428>.
- Andrew L. Maas, Awni Y. Hannun, and Andrew Y. Ng. Rectifier nonlinearities improve neural network acoustic models. In *in ICML Workshop on Deep Learning for Audio, Speech and Language Processing*, 2013.
- J. C. Mandel, D. A. Kreda, K. D. Mandl, I. S. Kohane, and R. B. Ramoni. SMART on FHIR: a standards-based, interoperable apps platform for electronic health records. *J Am Med Inform Assoc*, 23(5):899–908, 09 2016.
- Tomas Mikolov, Kai Chen, Greg Corrado, and Jeffrey Dean. Efficient estimation of word representations in vector space, 2013a.
- Tomas Mikolov, Quoc V. Le, and Ilya Sutskever. Exploiting similarities among languages for machine translation, 2013b.
- P. Nguyen, T. Tran, N. Wickramasinghe, and S. Venkatesh. Deepr: A convolutional net for medical records. *IEEE Journal of Biomedical and Health Informatics*, 21(1):22–30, 2017. doi: 10.1109/JBHI.2016.2633963.
- Adam Paszke, Sam Gross, Francisco Massa, Adam Lerer, James Bradbury, Gregory Chanan, Trevor Killeen, Zeming Lin, Natalia Gimelshein, Luca Antiga, Alban Desmaison, Andreas Kopf, Edward Yang, Zachary DeVito, Martin Raison, Alykhan Tejani, Sasank Chilamkurthy, Benoit Steiner, Lu Fang, Junjie Bai, and Soumith Chintala. Pytorch: An imperative style, high-performance deep learning library. In H. Wallach, H. Larochelle, A. Beygelzimer, F. d'Alché-Buc, E. Fox, and R. Garnett, editors, *Advances in Neural Information Processing Systems 32*, pages 8024–8035. Curran Associates, Inc., 2019. URL <http://papers.nips.cc/paper/9015-pytorch-an-imperative-style-high-performance-deep-pdf>.
- Jeffrey Pennington, Richard Socher, and Christopher D. Manning. Glove: Global vectors for word representation. In *Empirical Methods in Natural Language Processing (EMNLP)*, pages 1532–1543, 2014. URL <http://www.aclweb.org/anthology/D14-1162>.
- Tom J. Pollard, Alistair E. W. Johnson, Jesse D. Raffa, Leo A. Celi, Roger G. Mark, and Omar Badawi. The eICU Collaborative Research Database, a freely available multi-center database for critical care research. *Scientific Data*, 5(1): 180178, September 2018. ISSN 2052-4463. doi: 10.1038/sdata.2018.178. URL <https://doi.org/10.1038/sdata.2018.178>.
- L. Y. Pratt. Discriminability-based transfer between neural networks. In S. Hanson, J. Cowan, and C. Giles, editors, *Advances in Neural Information Processing Systems*, volume 5, pages 204–211. Morgan-Kaufmann, 1993. URL <https://proceedings.neurips.cc/paper/1992/file/67e103b0761e60683e83c559be18d40c-Paper.pdf>.
- Alvin Rajkomar, Eyal Oren, Kai Chen, Andrew M. Dai, Nissan Hajaj, Michaela Hardt, Peter J. Liu, Xiaobing Liu, Jake Marcus, Mimi Sun, Patrik Sundberg, Hector Yee, Kun Zhang, Yi Zhang, Gerardo Flores, Gavin E. Duggan, Jamie Irvine, Quoc Le, Kurt Litsch, Alexander Mossin, Justin Tansuwan, De Wang, James Wexler, Jimbo Wilson,

- Dana Ludwig, Samuel L. Volchenbom, Katherine Chou, Michael Pearson, Srinivasan Madabushi, Nigam H. Shah, Atul J. Butte, Michael D. Howell, Claire Cui, Greg S. Corrado, and Jeffrey Dean. Scalable and accurate deep learning with electronic health records. *npj Digital Medicine*, 1(1):18, December 2018. ISSN 2398-6352. doi: 10.1038/s41746-018-0029-1. URL <http://www.nature.com/articles/s41746-018-0029-1>.
- Laila Rasmy, Yang Xiang, Ziqian Xie, Cui Tao, and Degui Zhi. Med-bert: pretrained contextualized embeddings on large-scale structured electronic health records for disease prediction. *NPJ digital medicine*, 4(1):86, May 2021. ISSN 2398-6352. doi: 10.1038/s41746-021-00455-y. URL <https://europepmc.org/articles/PMC8137882>.
- Peter H. Schönemann. A generalized solution of the orthogonal procrustes problem. *Psychometrika*, 31(1):1–10, March 1966. ISSN 1860-0980. doi: 10.1007/BF02289451. URL <https://doi.org/10.1007/BF02289451>.
- Junyuan Shang, Cao Xiao, Tengfei Ma, Hongyan Li, and Jimeng Sun. Gamenet: Graph augmented memory networks for recommending medication combination. In *The Thirty-Third AAAI Conference on Artificial Intelligence, AAAI 2019, The Thirty-First Innovative Applications of Artificial Intelligence Conference, IAAI 2019, The Ninth AAAI Symposium on Educational Advances in Artificial Intelligence, EAAI 2019, Honolulu, Hawaii, USA, January 27 - February 1, 2019*, pages 1126–1133. AAAI Press, 2019. doi: 10.1609/aaai.v33i01.33011126. URL <https://doi.org/10.1609/aaai.v33i01.33011126>.
- Anders Søgaard, Sebastian Ruder, and Ivan Vulić. On the limitations of unsupervised bilingual dictionary induction. In *Proceedings of the 56th Annual Meeting of the Association for Computational Linguistics (Volume 1: Long Papers)*, pages 778–788, Melbourne, Australia, July 2018. Association for Computational Linguistics. doi: 10.18653/v1/P18-1072. URL <https://www.aclweb.org/anthology/P18-1072>.
- Nitish Srivastava, Geoffrey Hinton, Alex Krizhevsky, Ilya Sutskever, and Ruslan Salakhutdinov. Dropout: A simple way to prevent neural networks from overfitting. *Journal of Machine Learning Research*, 15(56):1929–1958, 2014. URL <http://jmlr.org/papers/v15/srivastava14a.html>.
- Ethan Steinberg, Ken Jung, Jason A. Fries, Conor K. Corbin, Stephen R. Pfohl, and Nigam H. Shah. Language models are an effective representation learning technique for electronic health record data. *Journal of Biomedical Informatics*, 113:103637, 2021. ISSN 1532-0464. doi: <https://doi.org/10.1016/j.jbi.2020.103637>. URL <https://www.sciencedirect.com/science/article/pii/S1532046420302653>.
- Shengpu Tang, Parmida Davarmanesh, Yanmeng Song, Danai Koutra, Michael W Sjoding, and Jenna Wiens. Democratizing EHR analyses with FIDDLE: a flexible data-driven preprocessing pipeline for structured clinical data. *Journal of the American Medical Informatics Association*, 0(0):14, 2020.
- Ashish Vaswani, Noam Shazeer, Niki Parmar, Jakob Uszkoreit, Llion Jones, Aidan N. Gomez, Lukasz Kaiser, and Illia Polosukhin. Attention is all you need, 2017.
- Barbara E. Wojcik, Catherine R. Stein, Raymond B. Devore, and L. Harrison Hassell. The Challenge of Mapping between Two Medical Coding Systems. *Military Medicine*, 171(11):1128–1136, November 2006. ISSN 0026-4075, 1930-613X. doi: 10.7205/MILMED.171.11.1128. URL <https://academic.oup.com/milmed/article/171/11/1128-1136/4578127>.
- Cao Xiao, Edward Choi, and Jimeng Sun. Opportunities and challenges in developing deep learning models using electronic health records data: a systematic review. *Journal of the American Medical Informatics Association*, 25(10):1419–1428, 06 2018. ISSN 1527-974X. doi: 10.1093/jamia/ocy068. URL <https://doi.org/10.1093/jamia/ocy068>.
- Zhen Xu, David R. So, and Andrew M. Dai. MUFASA: multimodal fusion architecture search for electronic health records. In *AAAI*, pages 10532–10540. AAAI Press, 2021.
- Chaohe Zhang, Xin Gao, Liantao Ma, Yasha Wang, Jiangtao Wang, and Wen Tang. Grasp: Generic framework for health status representation learning based on incorporating knowledge from similar patients. *Proceedings of the AAAI Confer-*

ence on Artificial Intelligence, 35(1):715–723, May 2021a. URL <https://ojs.aaai.org/index.php/AAAI/article/view/16152>.

Haoran Zhang, Natalie Dullerud, Laleh Seyyed-Kalantari, Quaid Morris, Shalmali Joshi, and Marzyeh Ghassemi. An empirical framework for domain generalization in clinical settings. In *Proceedings of the Conference on Health, Inference, and Learning, CHIL '21*, page 279–290, New York, NY, USA, 2021b. Association for Computing Machinery. ISBN 9781450383592. doi: 10.1145/3450439.3451878. URL <https://doi.org/10.1145/3450439.3451878>.

Appendix A. Additional justification of the motivation

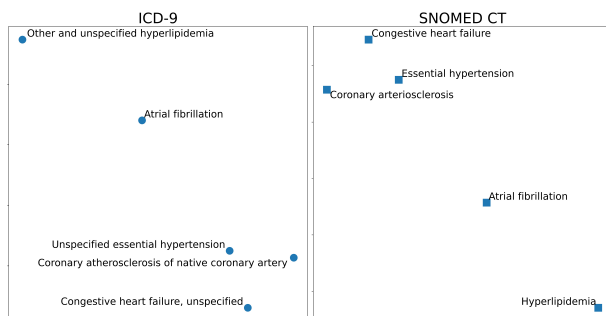


Figure 2: Distributed medical code embedding vectors in ICD-9 (left) and SNOMED CT (right). Note that “Coronary arteriosclerosis” in the right figure has synonyms “Arteriosclerotic heart disease”.

As shown in Fig. 2, we can see that these concepts have a similar structure in both spaces, suggesting that it is possible to learn an accurate mapping from one space to another. However, the task is non-trivial due to the following challenges.

- **Different granularities.** Different coding systems may have different granularities. For example, ICD-10 codes are known to be more specific than ICD-9 codes. As a result, there exist both one-to-one and one-to-many mappings.
- **Long-tail distribution.** The distribution of the frequencies of medical codes is often highly long-tailed. For example, in MIMIC-III (Johnson et al.,

2016) dataset, 50% of the codes appear less than a hundred times. Consequently, the medical code embeddings are quite noisy.

To tackle these two challenges, **AutoMap** learns the mapping across different coding systems in a coarse-to-fine manner. In this way, **AutoMap** can better align coding systems at different granularities and alleviate the long-tail distribution of the medical codes.

Appendix B. Notations

Notations used in this paper can be found in Tab. 6.

Notation	Meaning
V, v, \mathbf{c}	visit sequence, single visit, medical code
$\mathcal{O}, \mathcal{C}, \bar{\mathcal{C}}$	ontology, set of leaf/non-leaf codes
n, m	# of visits and codes
$\mathbf{e}, \mathbf{E}, d$	embedding vector, matrix, and dimension
$\phi(\cdot)$	code embedding mapping
$F(\cdot)$	backbone model
y, \hat{y}	labels and predictions
$*S, *T$	source and target dataset
$\text{ancestor}(\mathbf{c}, l)$	l -th level category for code \mathbf{c}
\mathbf{G}, \mathbf{D}	code groups and mapping dictionary
$\mathbf{M}, \bar{\mathbf{M}}$	original and sorted similarity matrix
l, k	grouping level and # of groups
$D(\cdot)$	discriminator
\cdot, \odot	matrix multiplication, Hadamard product
$[:, :]$	matrix indexing

Table 6: Notations used in this paper.

Appendix C. Jensen-Shannon Divergence

Jensen-Shannon divergence (JSD) can be seen as a symmetric version of Kullback–Leibler divergence (KLD), as in Eq. (13),

$$\text{JSD}(P\|Q) = \frac{1}{2} \left(\text{KLD}\left(P\|\frac{P+Q}{2}\right) + \text{KLD}\left(Q\|\frac{P+Q}{2}\right) \right),$$

$$\text{KLD}(P\|Q) = \sum_i P_i \log\left(\frac{P_i}{Q_i}\right).$$
(13)

Appendix D. Pseudo-Code

The pseudo-code of **AutoMap** can be found in Algo. 1.

Algorithm 1: AutoMap

```

/* S0: Embedding */
Obtain target code embeddings unsupervisedly
/* S1: Ontology-level Alignment */
Initialize empty dictionary  $\mathbf{D}^{(-1)}$ 
for  $l = 0, 1, \dots, \text{MaxDepth}$  do
    // Ontology Grouping
    Obtain  $l$ -th level coding groups  $\mathbf{G}_*^l$  (Eq. (2, 3))
    // Unsupervised Seed Induction
    Calculate similarity matrices  $\mathbf{M}_*^{(l)}$  (Eq. (4))
    Initialize mapping dictionary  $\mathbf{D}^{(l)}$  (Eq. (5))
    // Procrustes Optimization
    Merge dictionaries:  $\mathbf{D}^{(l)} = \mathbf{D}^{(l)} + \mathbf{D}^{(l-1)}$ 
    for number of iterative steps do
        Find optimal  $\mathbf{W}$  for current  $\mathbf{D}^{(l)}$  (Eq. (6))
        Induce new  $\mathbf{D}^{(l)}$  using optimal  $\mathbf{W}$  (Eq. (7))
    end
end
/* Step 2: Code-level Refinement */
for number of training iterations do
    Update discriminator  $D(\cdot)$  using Eq. (8)
    Update mapping matrix  $\mathbf{W}$  using Eq. (12)
end

```

Appendix E. Dataset

We select our cohort by filtering out the following samples: (1) patients younger than 18-year-old; (2) admissions without medical codes. For MIMIC-III (Johnson et al., 2016), due to the extreme long-tail distribution of medical codes, we further filter out medical codes that appear less than 50 times in the entire dataset. We split the data into source and target sets. (For Q1-3, this is done randomly. For Q4, this is based on hospital region). Each set is then split into training, validation sets with 0.7/0.1/0.2 ratio. There is no overlap of patients between any sets. The statistics of the two datasets can be found in Tab. 7.

Appendix F. Implementation Details

For the backbone models, we set the embedding dimension to 128. The detailed architectures are as follows:

- **MLP:** We first sum the code embeddings up and pass it through a linear layer with output dimension as 128 and ReLU activation to obtain the

	MIMIC-III (Johnson et al., 2016)	eICU (Pollard et al., 2018)
# of patients	6,444	11071
Gender	M: 3,583, F: 2,861	M: 6,209, F: 4,862
Age	64.1 ± 16.0	64.3 ± 15.8
# of visits	17,218	24,997
# of visits / patient	2.7 ± 1.7	2.2 ± 0.5
# of mortality patients	2,460	1,616
Length of stay (days)	10.7 ± 11.8	3.0 ± 4.8
# of ICD-9 codes	1,224	734
# of ICD-9 codes / visit	13.0 ± 6.4	4.3 ± 4.3
# of ICD-10 codes	-	682
# of ICD-10 codes / visit	-	4.2 ± 4.2
# of NDC codes	1,963	-
# of NDC codes / visit	41.1 ± 21.6	-

Table 7: Statistics of the datasets. M: male. F: female.

visit embedding. The visit embedding is then fed through a linear layer to obtain the prediction scores.

- **RNN:** We first sum the code embeddings up and pass it through the RNN layer with output dimension as 128 to obtain the visit embedding. The visit embedding is then fed through two linear layers with hidden dimensions as 128 and ReLU activation in between to obtain the prediction scores.
- **RETAIN (Choi et al., 2016a):** We follow the architecture described in the original work.
- **GCT (Choi et al., 2020):** We follow the architecture described in the original work. The original model does not support multiple visits. Thus, we add an RNN layer with output dimension as 128 at the top to model the temporal relation as suggested in the paper (Choi et al., 2020).
- **BEHRT (Li et al., 2020):** We follow the architecture described in the original work except that we stack 3 transformers layers with 2 attention heads as we find it works better with our dataset.

For the discriminator, we stack three linear layers with hidden dimensions as 128, leaky rectified linear function (LeakyReLU) (Maas et al., 2013), and Dropout (Srivastava et al., 2014) with a dropout rate 0.1 in between.

The model is selected based on the validation set, and the performance on the test set is reported. For mortality prediction and length-of-stay estimation, we use the cross-entropy loss. We use RMSprop as the optimizer. For the teacher-student framework in step 2, we optimize the discriminator five times, followed by the mapping for one time. For all baseline methods, we apply early-stopping with patience of 20 epochs by monitoring the validation AUC-PR

for mortality prediction and AUC-ROC for length-of-stay estimation.

The tunable hyper-parameters are batch size (8, 16, 32, 64), learning rate (1e-2, 5e-3, 1e-3, 5e-4, 1e-4), and loss coefficient α (0.1 - 0.9) in Eq. (12). We select the hyper-parameters using random search based on the validation set performance. The final selected hyper-parameters are: batch size with 8, learning rate with 1e-4, loss coefficient α with 0.1.

We implement `AutoMap` using PyTorch 1.6.0 (Paszke et al., 2019) and Python 3.8.5. The model is trained on an Ubuntu 20.04 machine with one AMD Ryzen Threadripper 3970X 32-Core CPU, 256GB memory, and two NVIDIA GeForce RTX 3090 GPUs.

Appendix G. Metrics

For mortality prediction (binary classification), we report Area Under the Receiver Operating Characteristic Curve (ROC-AUC) scores and Area Under the Precision Recall Curve (PR-AUC) scores. For length-of-stay estimation (multi-class classification), we report weighted one-v.s.-one ROC-AUC score and weighted F1 scores.

For code mapping evaluation, we report similarity and hit@10. Similarity measures the mean cosine similarity of the transformed code embeddings between the ground truth mapping pairs. Hit@10 measures the proportion of mapped codes in the top-10 set that are correct.

For metrics ROC AUC, PR AUC, and F1, we report the average scores and standard deviation of bootstrapping for 1000 times. For similarity and hit@10 metrics, we report the average scores and standard deviation of results from three random seeds. We perform independent two-sample t-test to evaluate if `AutoMap` achieves significant improvement over baseline methods.

Appendix H. Additional Experiments

H.1. Additional Results for Q1: Target Data with Limited Labels

H.2. k-Means Grouping

We provide additional experiments in Tab. 9. `AutoMap` (k-Means) uses k-Means instead of ontology to group the medical codes in step 1 (ontology-level alignment). We can see that `AutoMap` (k-Means) can

Backbone	Method	Mortality AUC-ROC	Length-of-Stay AUC-ROC
MLP	<i>Full-Label</i>	<i>0.6531 ± 0.0232</i>	<i>0.2819 ± 0.0317</i>
	Direct Training	0.6191 ± 0.0237	0.5345 ± 0.0184
	Transfer Learning	0.6240 ± 0.0240	0.6095 ± 0.0140
	MUSE	0.6276 ± 0.0236	0.6240 ± 0.0157
	VecMap	0.6502 ± 0.0231	0.6341 ± 0.0159
	AutoMap	0.6631 ± 0.0228*	0.6350 ± 0.0160
RNN	<i>Full-Label</i>	<i>0.6539 ± 0.0231</i>	<i>0.2818 ± 0.0319</i>
	Direct Training	0.5547 ± 0.0249	0.4427 ± 0.0174
	Transfer Learning	0.6234 ± 0.0235	0.6166 ± 0.0140
	MUSE	0.6260 ± 0.0231	0.6367 ± 0.0159
	VecMap	0.6488 ± 0.0226	0.6416 ± 0.0153
	AutoMap	0.6627 ± 0.0223*	0.6487 ± 0.0161*
RETAIN	<i>Full-Label</i>	<i>0.6190 ± 0.0244</i>	<i>0.2648 ± 0.0302</i>
	Direct Training	0.5466 ± 0.0266	0.4427 ± 0.0174
	Transfer Learning	0.5732 ± 0.0251	0.5395 ± 0.0170
	MUSE	0.5838 ± 0.0252	0.5831 ± 0.0207
	VecMap	0.6315 ± 0.0239	0.5963 ± 0.0200
	AutoMap	0.6528 ± 0.0234*	0.6007 ± 0.0188*
GCT	<i>Full-Label</i>	<i>0.6533 ± 0.0240</i>	<i>0.2814 ± 0.0323</i>
	Direct Training	0.5402 ± 0.0239	0.4865 ± 0.0166
	Transfer Learning	0.5967 ± 0.0235	0.5718 ± 0.0146
	MUSE	0.6016 ± 0.0232	0.6129 ± 0.0153
	VecMap	0.6291 ± 0.0228	0.6085 ± 0.0149
	AutoMap	0.6539 ± 0.0229*	0.6363 ± 0.0147*
BEHRT	<i>Full-Label</i>	<i>0.6673 ± 0.0219</i>	<i>0.2652 ± 0.0275</i>
	Direct Training	0.5438 ± 0.0226	0.4730 ± 0.0175
	Transfer Learning	0.6190 ± 0.0233	0.5609 ± 0.0153
	MUSE	0.6040 ± 0.0227	0.5869 ± 0.0191
	VecMap	0.6740 ± 0.0223	0.6044 ± 0.0173
	AutoMap	0.6737 ± 0.0220	0.6328 ± 0.0178*

Table 8: Additional results with limited labeled data in the target site (same setting as Tab. 1).

Method	Mortality AUC-PR	Length-of-Stay F1
<code>AutoMap</code> (k-Means)	0.2520 ± 0.0269	0.3605 ± 0.0179
AutoMap	0.2712 ± 0.0280*	0.3744 ± 0.0182*

Table 9: Additional experiments in the scenario where the ontology is not available. Experiment results show that `AutoMap` can adapt to the case where the medical ontology is not available.

achieve similar performance to `AutoMap` using ontology (though not as good). This shows that `AutoMap` can adapt to the case where the medical ontology is not available.

H.3. Sufficient Labeled Data Scenario

We further evaluate `AutoMap` in the scenario where the target site has sufficient labeled data. We note that this scenario is less practical in the real world, as the target site may often be some small health in-

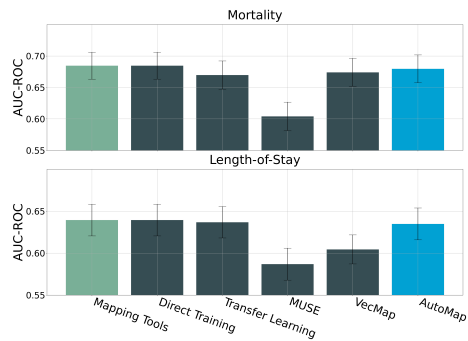


Figure 3: Results with sufficient labeled data in the target site. Error bar denotes standard deviations. Experiment results show that **AutoMap** can achieve comparable or even better performance with sufficient labeled data. Note that this scenario is less practical in real world and is not the intended usage for **AutoMap**.

stitution with limited labeled data. The results can be found in Fig. 3. In this scenario, direct training and transfer learning baselines can significantly improve since the labeled data is sufficient. Further, we can see that the code mapping tools baseline is quite strong due to the utilization of external resources. Despite these, we can see that **AutoMap** still achieves comparable or even better performance with sufficient labeled data.